Ir^{III} as a Strategy for Preorganization in H-bonded Motifs

Barbora Balónová,[a] Helena J. Shepherd,[b] Christopher J. Serpell,[b] Barry A. Blight*[a,b]

[a] *University of New Brunswick, Department of Chemistry, Fredericton, New Brunswick, Canada, E3B 5A3*

[b] *School of Physical Sciences, University of Kent, Canterbury, United Kingdom, CT2 7NH*

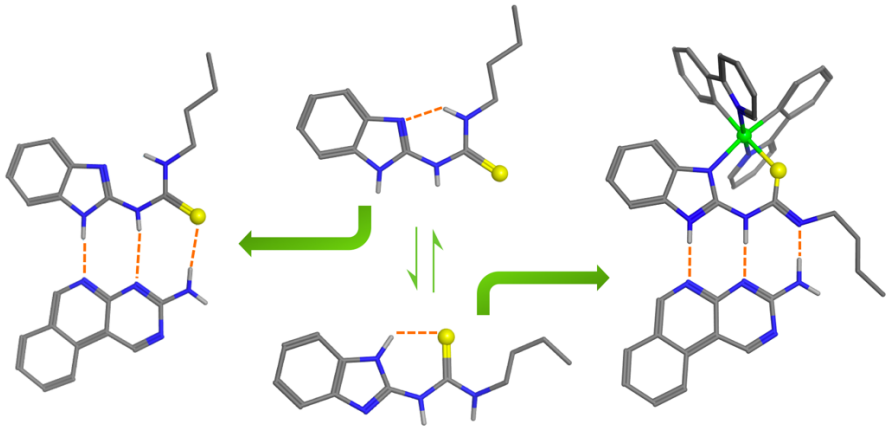

ABSTRACT Here we present the synthesis and characterisation of four hydrogen bonded systems based on thiourea derivatives. These motifs are considered to be stable and desirable for supramolecular hydrogen-bonded functional materials. Interpretation of the structural design of thiourea based ligand and its incorporation into metal complexes can contribute to the understanding of preorganised self-assembly and open new pathways in design of novel soft materials. This work contributes to the unexplored library of hydrogen bonded metal complexes based on iridium. Further we examined the photoluminescence of the system of general formula $[Ir(C^N)_2(N^S)]$ and the effect of hydrogen bonding on the emission properties when combined with different *n*-heteroacenes.

INTRODUCTION

Hydrogen bonds are ubiquitous interactions in self-assembly and critical for secondary, tertiary and quaternary biological structure.[1,2] They have been extensively used for the construction of

supramolecular systems since they are highly selective, directional, and moderately strong.[3,4] They are formed when an acceptor atom (A) carrying a non-bonding electron pair is interacting with donor atom (D) with an available acidic hydrogen atom. The binding strength depends mainly on the solvent environment and the multiplicity of H-bonds.[5] Multiple H-bonding interactions are important in host-guest chemistry (e.g. recognition of urea[6]). There are many examples of double,[7,8] triple,[9-12]and quadrupole[13] hydrogen bonded systems. The triple H-bonded complexes with a linear array AAA-DDD are treated as very strong (association constant in solvents such as chloroform typically exceed $10^5 M^{-1}$) and stable among the sequences.[14,15] The strength of these systems is a result of the secondary interactions.[16,17] The first example of AAA-DDD complex was discovered in 1992 by Zimmerman and Murray,[18] but unfortunately, the components were unstable at room temperature and susceptible to tautomerization.[19] More recent studies on triple H-bonded systems described a flexible methods for the synthesis of novel triple H-bonded motifs[20,21] based on relatively planar rigid conformations, but non-coplanar systems have been also investigated.[22]

The binding abilities of thiourea derivatives have been previously investigated for their anion complexation properties,[23-25] for example, to bind phosphate in water,[26] and for sensing of nerve agents.[27] Moreover, the thiourea moiety has been implemented into hydrogels, used as anion transporters through membranes,[28] and for sensor materials.[29] In this study we describe

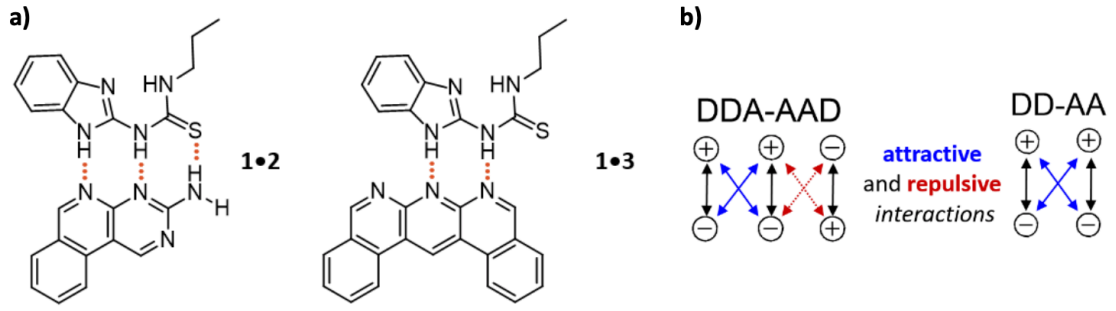

Figure 1 a) Designed motifs **1•2** and **1•3** of self-assembling triple hydrogen bonded systems. **b)** Secondary electrostatic interactions in H-bonded systems **1•2** and **1•3**. Attractive and repulsive interactions showed in blue and red arrows, respectively.

the design, characterization, and binding studies of easily accessible H-bonded motifs employing thiourea derivative **1** as a hydrogen bond compliment to hetero-fused-*n*-acenes **2** and **3** (Figure 1). We were interested in exploring the strength and specificity of these units and the potential enhancement of the association strength after conversion of compound **1** into novel neutral iridium-chelate complex **4** (Figure 2). The presence of the metal within the structure inhibited the free rotation of the thiourea ligand **1** resulting in better control over the structural alignment for the H-bonded systems.

Most iridium (III) complexes are based on N^N, O^O, N^O coordination framework[30-34] while the sulfur atom is very rarely exploited, although it is known that the S atom has advantages as large atomic radius and easy coordination with transition metals,[35] novel iridium complexes containing four-membered rings (with Ir-S-P-S and Ir-S-C-S structures) were recently reported.[36,37] In this paper, complex **4** with general formula [Ir $(C^N)_2(N^S)$], represents the first example of an iridium complex bearing benzimidazolyl thiourea ligand **1**, which is also capable of creating a higher-order structures. Here, we compare the association of four different heterodimeric systems through ^{1}H NMR, UV-Vis analysis. Furthermore, the influence of H-bonding on emission properties of iridium complex **4** is reported.

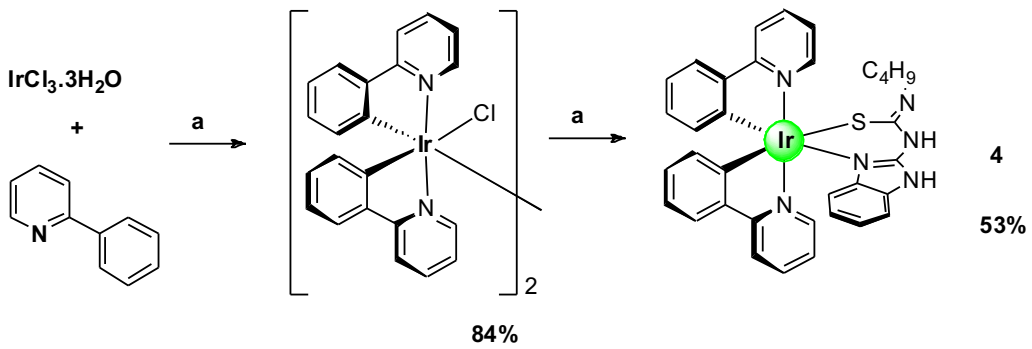

Figure 2. The synthetic route of Ir (III) complex **4**. Reagents and conditions: a) 2-ethoxyethanol:water (3:1), reflux, 24h; b) 1-(1H-Benzo[d]imidazole-2-yl)-3-butylthiourea, K_2CO_3, toluene, N_2 (g).

EXPERIMENTAL SECTION

Materials. All starting materials were purchased from commercials sources and used as received without further purification unless otherwise noted. Analytical thin layer chromatography was done on precoated TLC plates Alugram Sil G/UV254. Column chromatographic purifications were done with silica gel, ultrapure, 60-200 μm (60 Å) or aluminium oxide (activated, neutral) as specified. All experiments were performed under a dry N_2 atmosphere using standard Schlenk techniques unless otherwise noted.

NMR. ^{1}H (400 MHz) and ^{13}C (100 MHz) NMR spectra were recorded on a "JEOL ECS 400" spectrometer in deuterated solvents such as chloroform-*d*, DMSO-d_6 as noted. All chemical shifts are reported in δ (ppm) referenced to tetramethylsilane, Si $(CH_3)_4$, while peak multiplicities are referred to as singlet (s), doublet (d), triplet (t), quartet (q), broad singlet (bs), and multiplet (m).

Mass Spectrometry, Elemental, and Melting Point Analyses. High-resolution mass spectral data measurements were performed by the Mass Spectrometry Laboratory, Dalhousie University, Halifax, Canada. High-resolution mass spectra were recorded on Bruker Daltonics MicrOTOF Instrument. The ionization method used for low-res and high-res analysis was positive or negative electrospray ionization (ESI). The sample was introduced by a syringe pump at flow rate of 2 µL/min. The spray voltage applied to the ESI needle is 4.5kV. The dry gas flow rate was 4 L/min. Nebulizer gas was 1 Bar and source temperature was 180 °C. Elemental analysis was performed by the Centre for Environmental Analysis and Remediation, Saint Mary's University, Halifax, Canada. Carbon, hydrogen and nitrogen analyses were carried out on a Perkin Elmer 2400 Series II CHN Analyser. Results are obtained as a percentage by weight and are measured as a function of thermal conductivity. For the

microanalysis sample sizes were between 2.5-3.5 mg. Melting points were determined on Buchi Melting Point Instrument.

UV-Visible Absorption. Absorption spectra were recorded at room temperature using Agilent Cary 4000 UV-Vis double beam spectrophotometer.

Photoluminescence Analyses. Steady-state emission and excitation spectra and time-resolved emission spectra were recorded at 298 K using an Edinburgh Instrument FS5. All samples for steady-state measurements were excited at 360 nm and the samples for time-resolved measurements at 363 nm using Pulsed LED-365 nm diode laser. Photoluminescence quantum yields were determined through direct method using the integrating sphere. Further details of all PL analyses are available in the Supporting Information section S5.

Single Crystal X-ray Diffraction. Suitable crystals were grown by slow vapour diffusion of hexanes into a solution of **1**, **1•2/3** dissolved in $CHCl_3$ and mounted on a Rigaku Oxford Diffraction Supernova diffractometer. The data were refined by least-squares minimization using ShelXL[38] and solved by intrinsic phasing using ShelXT.[39] Olex2[40] was used as an interface to all ShelX programs. CCDC 1935520, 1935521, 1935522 and 1935523 contain the supplemental crystallographic information and are available free of charge from the Cambridge Crystallographic Database.

Crystal Data for $C_{12}H_{16}N_4S$ **1** (M =248.35 g/mol): monoclinic, space group C2/c, a = 29.7869(8) Å, b = 4.44193(11) Å, c = 19.2530(5) Å, β = 107.232(3)°, V = 2433.05(12) $Å^3$, Z = 8, T = 100.00(10) K, μ(CuKα) = 2.220 mm^{-1}, Dcalc = 1.356 g/cm^3, 16716 reflections measured (6.214° ≤ 2Θ ≤ 145.746°), 2397 unique (Rint = 0.0394, Rsigma = 0.0233) which were used in all calculations. The final R1 was 0.0292 (I > 2σ(I)) and wR2 was 0.0715 (all data).

Crystal Data for $C_{11}H_8N_4$ **2** (M =196.21 g/mol): triclinic, space group P1, a = 7.2852(6) Å, b = 7.6006(6) Å, c = 9.4873(7) Å, α = 74.100(6)° ® = 86.330(6)°, γ = 61.450(8)°, V = 442.40(7) Å^3, Z = 2, T = 100.00(10) K, μ(CuKα) = 0.762 mm^{-1}, Dcalc = 1.473 g/cm^3, 16716 reflections measured (6.214° ≤ 2Θ ≤ 145.746°), 2397 unique (Rint = 0.0394, Rsigma = 0.0233) which were used in all calculations. The final R1 was 0.0292 (I > 2σ(I)) and wR2 was 0.0715 (all data).

Crystal Data for $C_{23}H_{24}N_8S$ **1•2** (M =444.56 g/mol): monoclinic, space group P21/n, a = 13.2112(6) Å, b = 4.9417(2) Å, c = 32.3534(12) Å, β = 90.456(4)°, V = 2112.13(15) Å^3, Z = 4, T = 100.00(10) K, μ(CuKα) = 1.598 mm^{-1}, Dcalc = 1.398 g/cm^3, 7285 reflections measured (5.464° ≤ 2Θ ≤ 133.194°), 3528 unique (Rint = 0.0409, Rsigma= 0.0520) which were used in all calculations. The final R1 was 0.0393 (I > 2σ(I)) and wR2 was 0.0945 (all data).

Crystal Data for $C_{31}H_{27}N_7S$ **1•3** (M =529.65 g/mol): monoclinic, space group P21/n, a = 7.23003(11) Å, b = 26.3191(4) Å, c = 13.59163(19) Å, β = 91.7138(14)°, V = 2585.17(6) Å^3, Z = 4, T = 100.00(10) K, μ(CuKα) = 1.390 mm^{-1}, Dcalc = 1.361 g/cm^3, 18595 reflections measured (6.716° ≤ 2Θ ≤ 146.052°), 5083 unique (Rint = 0.0495, Rsigma = 0.0362) which were used in all calculations. The final R1 was 0.0476 (I > 2σ(I)) and wR2 was 0.1321 (all data).

Host-Guest Titrations. All dilutions and titrations were performed using Hamilton Gastight microliter syringes at room temperature. ^{1}H NMR dilution studies of compounds **1**, **2** and complex **4** were performed in $CDCl_3$ or $CDCl_3$/ DMSO-d_6 mixture (99:1) with additions of appropriate aliquots of solvent. UV-Vis dilution studies of compounds **1**, **2** and complex **4** were performed in HPLC grade chloroform with addition of appropriate aliquots of HPLC grade chloroform. NMR titration studies were performed with host (10^{-3} M) and titrated with the addition of appropriate aliquots of a solution of guest (10^{-2} M) with a background concentration

of host to maintain a constant concentration of host throughout the study. UV-Vis titration studies were performed with host (10^{-5} M) and titrated with the addition of appropriate aliquots of a solution of guest (10^{-4} M) with or without a background concentration of host. Further details about titration experiments are available in the Supporting Information section S3 and S4. All dilution and titration data were analysed with the program BindFit.[41]

Synthesis.

Iridium complex 4. Iridium dimer complex **$[Ir(ppy)_2Cl]_2$** (145 mg, 1.35 x 10^{-4} mol),[42] 1-(1H-benzo[d]imidazol-2-yl)-3-butylthiourea **1** (83 mg, 2.5 equiv.), and potassium carbonate (184 mg, 10 equiv.) were added to 15 mL of dry toluene. Nitrogen was bubbled through the reaction mixture for 15 min and then the reaction was refluxed for 22 h under N_2 atmosphere. After cooling down to room temperature, the solvent was removed under reduced pressure and dichloromethane (20 mL) was added to dissolve the solid. The mixture was extracted with water (3 x 20 mL) to remove the excess base. The organic layers were combined, dried over magnesium sulphate and the solvent was removed under reduced pressure. Product was further purified via precipitation (chloroform/hexane) and dried under vacuum for 24 h. Final product **4** was obtained as bright yellow powder in 53 % yield.

^{1}H NMR (400 MHz, 298 K, $CDCl_3$) δ (ppm): 9.58 (bs, 1H), 8.47 (bs, 1H), 8.36 (d, 1H), 7.87 (d, 1H), 7.72 (d, 1H), 7.67 (t, 1H), 7.60-7.56 (m,2H), 7.01 (t, 1H), 6.92-6.80 (m, 4H), 6.72 (t, 1H), 6.58 (t, 1H), 6.45 (d,1H), 6.22 (d, 1H), 5.64 (bs, 1H), 3.40 (m, 2H), 1.53 (m, 2H), 1.34 (m, 2H), 0.91 (t, 3H). **^{13}C NMR** (100 MHz, 298 K, $CDCl_3$) δ (ppm): 168.42, 151.20, 150.47, 144.18, 143.79, 136.42, 136.00, 132.15, 131.62, 129.69, 129.61, 124.34, 123.95, 121.84, 121.57, 121.10, 120.98, 118.94, 118.53, 117.85, 108.47, 77.36, 31.74, 20.26, 13.99. **ESI-HRMS** calculated: 749.2033. Found: 749.2038 [M+]. **Anal. Calcd** for $C_{34}H_{31}IrN_6S$: C, 54.60; H, 4.18; N, 11.24. Found: C, 54.26; H, 4.11; N, 11.22.

Results and Discussion Synthesis for compound **1** is known[43] but was slightly modified and can be found in our previous work[44] together with the synthetic procedure for compound **2**. Compound **3** was prepared by reacting 3, 5-diiodopyridine-2, 6-diamine[45] with 2-formylphenylboronic acid, following tandem Suzuki-Miyaura cross-coupling / imine condensation / cyclization procedure published by the Leigh Group.[46] Complex **4** was synthesised by refluxing 1-(1H-benzo[d]imidazol-2-yl)-3-butylthiourea **1** with the iridium μ-chloro-bridged dimer $[Ir(ppy)_2Cl]_2$ (ppyH = phenylpyridine) in the presence of an excess base in toluene. Isolation after purification, yielded **4** as a yellow solid.

Single crystals of compound **1** and **2** (Figure 3), and co-crystals of **1•2** and **1•3** (Figure 4) suitable for X-ray diffraction study were obtained by slow vapour diffusion of hexanes into a chloroform solution of **1**, **2** and **1•2**/**1•3**, respectively. Compound **1** (Figure 3a) belongs to the C2/c space group (monoclinic) with 8 molecules per unit cell. All crystal parameters of this

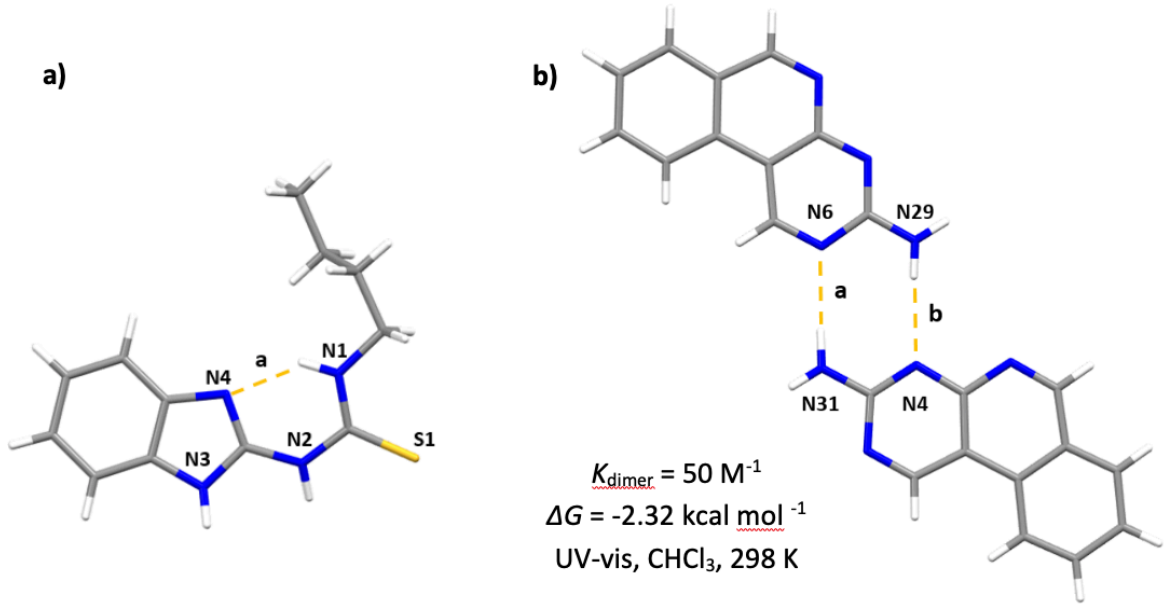

Figure 3 a) X-ray crystal structure of compound **1** with annotated NH···N contacts (orange); (a) N4···N1 = 2.69 Å, NH···N = 141°. **b)** X-ray crystal structure of compound **2** with annotated NH···N contacts (orange); (a) N6···N31 =2.97 Å, NH···N =177°; (b) N29···N4 = 3.04 Å, NH···N =167°.

compound can be found in Supporting Information, section S6. As expected, an intramolecular hydrogen contact between atoms N4 and N1 was observed (a = 2.69 Å, NH···N = 141°). We compared the parameters of the mentioned contact in the co-crystal structures, where we observed that addition of different binding partners (**2**, **3**) can influence the geometry in the crystal structure of compound **2**. A suitable crystal of compound **2** for X-ray analysis was obtained after synthesis and crystallized as a H-bonded dimer, as expected (Figure 3). We were interested in the observed intramolecular N6···N31 and N29···N4 contact distances (*a* = 2.97 Å, *b* = 3.04 Å), which are less than the sum of van der Waals radii[47] characteristic for this type of interaction.

Single crystals of the **1•2** neutral DDA-AAD and **1•3** DD-AA were obtained by slow diffusion of hexane into a concentrated solution of **1•2/ 1•3** in chloroform. X-ray diffraction analysis revealed that the triple hydrogen bonded **1•2** system crystallized in space group $P2_1/n$ with 4 molecules per unit cell. The structure (Figure 4a) showed a planar array of intermolecular NH···N (b= 2.81 Å, c= 3.20 Å) and NH···S (c= 3.25 Å) contacts. The intramolecular hydrogen contact between N1···N3 was still present (a= 2.67 Å) in the structure with a slightly shorter bond length and NH···N angle due to binding of the guest molecule **2**. As expected, the fused pyrimido[4,5-*c*]isoquinolin-3-amine **2** holds the AAD binding site of the system planar in the DDA-AAD **1•2** arrangement, which is confirmed by the angle values (b=179°, c=172°) that are not far from the ideal value of 180°**,** which is typical for the strongest types of H-bonds.[4]

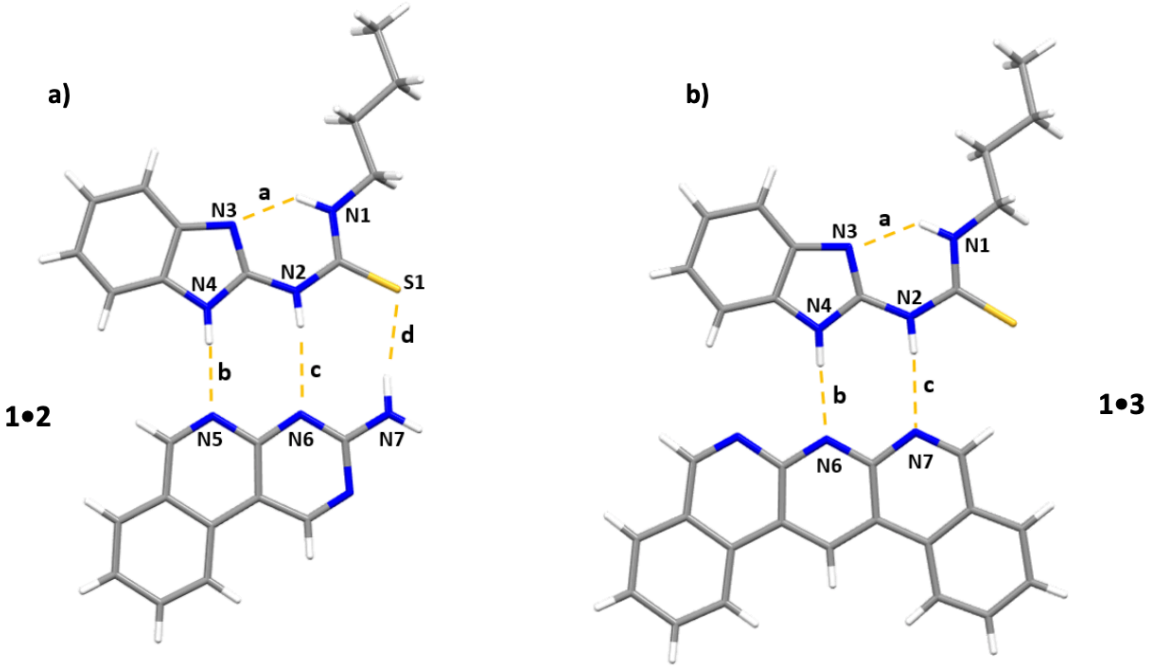

Figure 4. a) X-ray crystal structure of co-crystal **1•2** with annotated NH···N and NH···S contacts (orange); (a) N1···N3 =2.67 Å, NH···N =138°; (b) N4···N5 = 2.81 Å, NH···N =179°; (c) N2···N6 =3.20 Å, NH···N =172°; (d) S1···N7 = 3.25 Å, NH···S =170°. **b)** X-ray crystal structure of co-crystal **1•3** with annotated NH···N (orange); (a) N1···N3 =2.71 Å, NH···N =139°; (b) N4···N6 = 2.89 Å, NH···N =177°; (c) N2···N7 =2.98 Å, NH···N =175°.

The solid-state structure of **1•3** is similar to **1•2** system. In this case, the X-ray diffraction analysis of system **1•3** indicated the presence of two intermolecular hydrogen bond interactions in DD-AA alignment (Figure 4b). This double hydrogen bonded array crystallized in monoclinic $P2_1/n$ space group including four molecules per unit cell. The participation of known benzo[*f*]isoquinolino[3,4-*b*][1,8]naphthyridine **3**[46] as a binding partner in **1•3** array improved the planarity of system (b = 177°, c= 175°) and shortened the H-bond length in comparison with system **1•2** (Δ = 0.22 Å) within molecule (N2···N7, c = 2.98 Å) was observed. The major contrast between these two systems is the lack of a hydrogen bond facilitated by the sulphur S1 in the **1•3** system, which is not reaching the sufficient distance for the concomitantly weak C-H contact.

The dimerization behaviour of compound **2** was also studied by using ^{1}H NMR spectroscopy, where the observed NH_2 protons were slightly shifted upfield revealed the K_d = 60 M^{-1} ± 6%

($CDCl_3$/DMSO-d_6, 99:1, 298 K) (see Supporting Information, section **S3**) as a result of weak self-association. As the solubility of compound **2** is inherently poor (due to the existence of hydrogen bonds within the molecule and its self-association tendency), 1% addition of DMSO-d_6 in chloroform-*d*, was used to support the solubility of compound **2** during NMR analysis. This value was further confirmed by UV-Vis analysis in chloroform (K_d =50 M^{-1} ± 0.3%, 298K, see Supporting Information, section **S4**). The value of the dimerization constant for compound **2** suggests that a minimal destructive energy is required in order to disassemble the self-associated dimer in chloroform to form the proposed H-bonded systems **1•2** and **4•2**.

The H-bonded co-system **1•2** can be described as a DDA-AAD array. The strength of this interactions was examined by ^{1}H NMR spectroscopy (Figure 5) and UV-vis analysis. The downfield shifts of the NH_2 protons in **2** agreed with the formation of co-system **1•2** as designed, revealing the association constants K_{11} = 2.7 x 10^3 M^{-1} ± 5%, K_{12} = 1.3 x 10^2 M^{-1} ± 1% (^{1}H NMR, $CDCl_3$/ DMSO-d_6, 99:1, 298K). The 1:2 stoichiometry which was confirmed by job plot analysis (Figure S8). The strength of the H-bonding interactions in co system **1•2** was determined by UV-vis titration analysis in HPLC grade chloroform with 1% of DMSO,

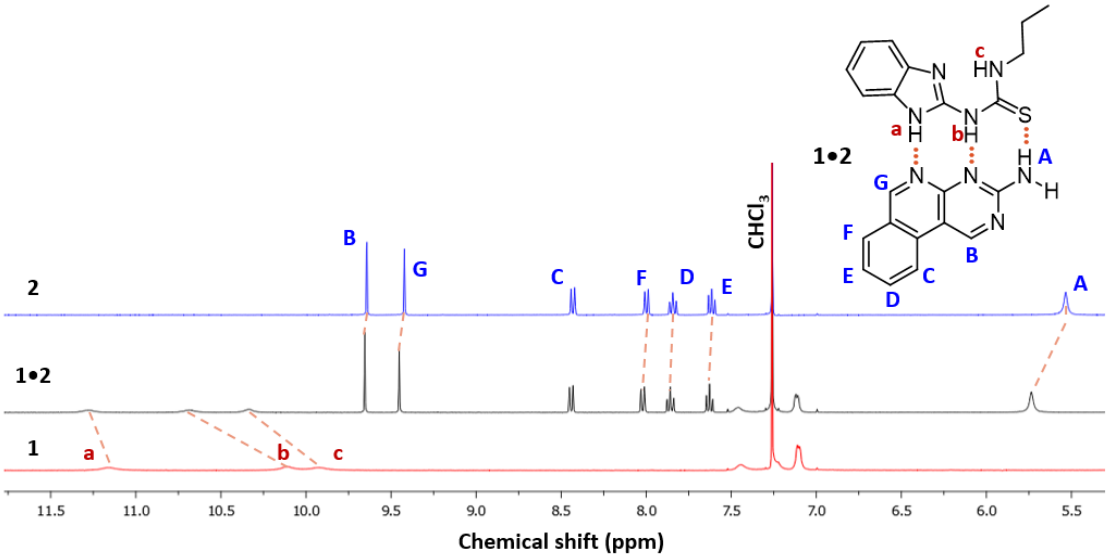

Figure 5. Partial ^{1}H NMR (400MHz, $CDCl_3$, 298K) of **2** (blue), complex **1•2** (black), and **1** (red). Dashed orange lines show shifts upon formation of complex **1•2**.

revealing an association constants K_{11} = 2.6 x 10^4 M^{-1} ± 0.4%, K_{12} = 1.4 x 10^4 M^{-1} ± 0.4% (UV-Vis, $CHCl_3$/ DMSO, 99:1, 298K), for the 1:2 stoichiometry of **1•2**. Change in the absorbance revealed a higher association constant for both **1•2** in comparison with the NMR studies of these systems. We postulate that increased number of π-π stacking interactions within the systems during the NMR binding studies (concentration requirement 10^{-2} to 10^{-3} M), which is suppressed in lower concentrations used for UV-vis analysis (10^{-5} M), is the root cause of this phenomena.

The H-bonded co-system **1•3** can be described as DD-AA double H-bonded array, with two attractive interactions within the structure. Proton shifts observed during the NMR analysis led to K_a = 1.6 x 10^3 M^{-1} ± 12% (^{1}H NMR, $CDCl_3$/ DMSO-d_6, 99:1, 298K) for the **1•3** co-system (Figure 6). This interaction was examined for lower concentrations through UV-vis analysis with much lower error for fitting. The association constant for **1•3** system proved to be K_a = 7.0 x 10^2 M^{-1} ± 0.2% (UV-Vis, $CHCl_3$/ DMSO, 99:1, 298K).

As expected, compound **1** binds much stronger with partner **2** (two orders of magnitude stronger) than it binds **3**. The extra H-bond between the donor N-H group and sulphur in **1•2** raises its stability over **1•3.** The structural organisation and multiplicity for the host-guest assembly clearly plays a role in affecting the strength of the multipoint hydrogen bonded system. (See Supporting Information sections S3 and S4 for further details of NMR and UV-vis titration experiments).

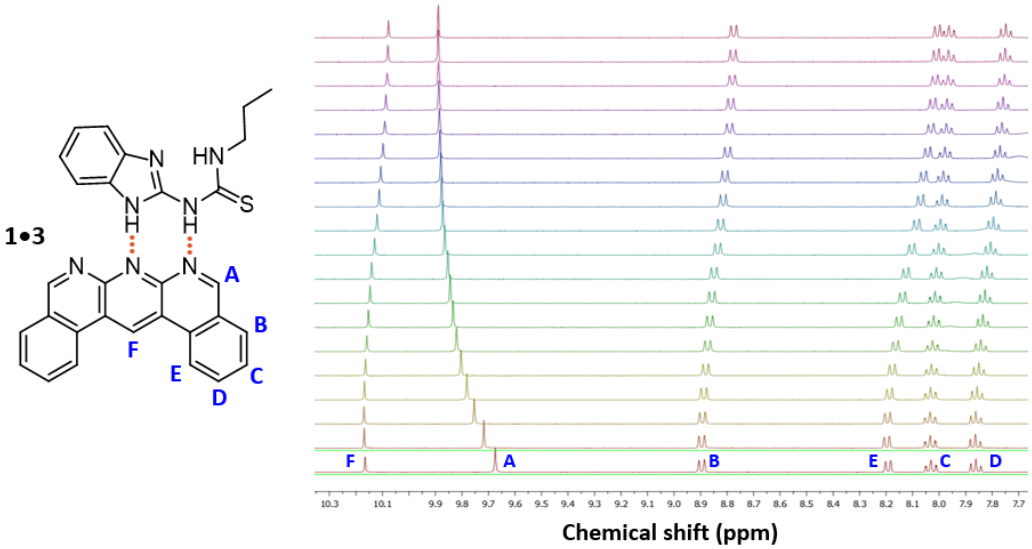

Figure 6. Partial stacked ^{1}H NMR (400MHz, $CDCl_3$, 298K) from titration experiment for **1•3** system in $CDCl_3$/DMSO-d_6, 99:1, 298 K with the observed change in the chemical shift.

Complex **4** is similar in structure to our previously reported iridium complex[44] which crystallized in the triclinic space as an H-bonded dimer, bearing a benzimidazolyl-guanidine ligand. Single crystals of complex **4** were not attainable, however we nonetheless analysed the possible formation of an H-bonded iridium dimer in solution using ^{1}H NMR spectroscopy (see Supporting Information, section S3). There was no proton shift observed during the dilution experiment of **4** in chloroform-*d*, which is indicating that complex **4** does not noticeably self-associate. In this case incorporation of compound **1** into heteroleptic iridium complex **4** is suppressing the free rotation of ligand **1**, leading to a pre-organized arrangement for complexation with compounds **2** and **3** (Figure 7). Compound **4** was separately paired with guests **2** and **3** and examined through ^{1}H NMR analysis and UV-vis binding studies to quantify their respective association constants and compared with non-metal systems **1•2** and **1•3**.

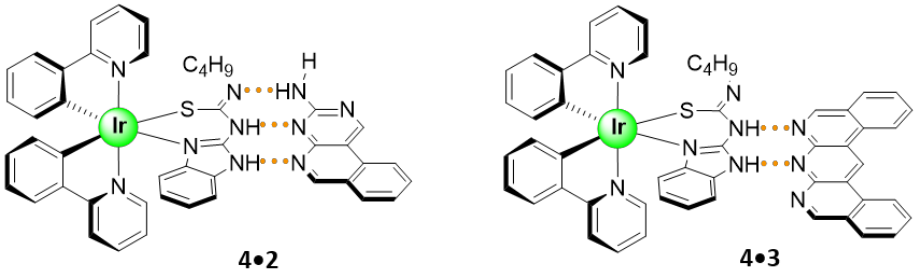

Figure 7. Structures of neutral iridium complex **4** with *n*-heteroacenes (**2**, **3**). Primary hydrogen bonding interactions for co-systems **4•2** and **4•3** are annotated as orange dotted lines.

The co-system **4•2** can be described as triple bonded ADD-DAA motif with two attractive and two repulsive interactions within the structure. The strength of this interaction was assessed by UV-Vis absorption titration (Figure 8) of **4** with **2** ($CHCl_3$ / DMSO, 99:1), revealing an association constant K_a = 2.1 x10^3 M^{-1} ± 0.2% and the binding energy of 4.5 kcal mol^{-1}. System **4•2** is comparable with our previously reported ADD-DAA system[44] where the studied iridium complex was bearing a benzimidazolyl-guanidine ligand. As expected, guanidine-based complex revealed a higher association constant for binding with compound **2** (K_a = 4.3 x10^3 M^{-1}, UV-vis, $CHCl_3$ / DMSO, 98:2) than complex **4**. The increased association constant is ascribed to higher acidity (guanidine pKa = 13.6, thiourea pKa =21.0)[49] and higher hydrogen-bond donating ability of guanidine derivatives. In these instances, the inclusion of the iridium(III) centre plays two roles. Firstly, it allows for the inclusion of a metal centre that is accompanied by a number of well documented physical,[50-51] photophysical,[52-55] and catalytic properites.[56-58] Second, and more relevant to this study, is the inherent stabilization provided by the removal of energetically destructive rotational isomerization. Using the Sartorius empirical model, **4•2** is calculated to be 5.7 kcal mol^{-1}, however the 1.2 kcal mol^{-1} shortfall can be accounted with the competitive solvent choice required to analyse this system.[15]

Compound **3** has been previously reported to improve stability and give high association constants with appropriate binding partners in AAA-DDD complexes.[59] The neutral complex **4** formed a double hydrogen bonded array with **3** in DD-AA array. From the UV-Vis titration experiment of **4** with **3** the association constant was determined to be K_a = 1.6 x10^3 M^{-1}± 0.1% ($CHCl_3$ / DMSO, 99:1) and as predicted, the lowest from all four studied iridium co-systems.

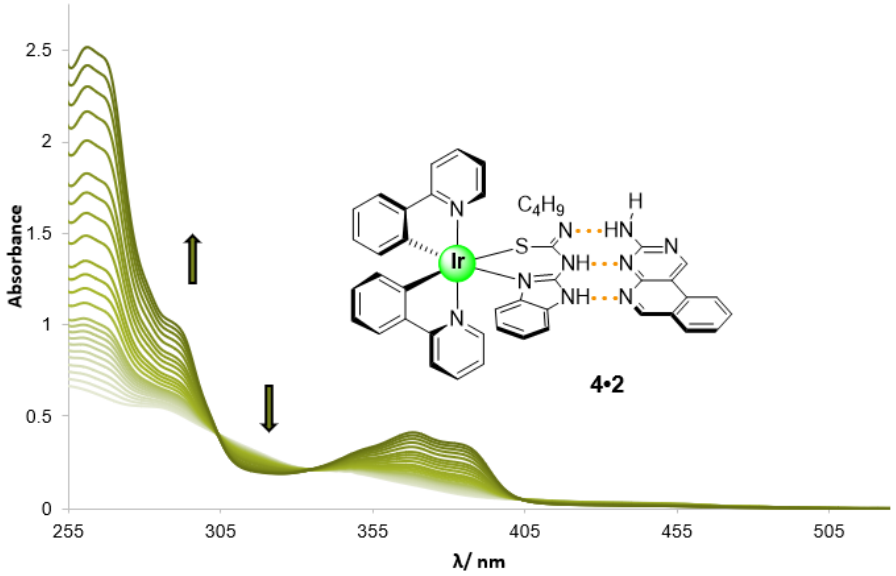

Figure 8 Results from the UV-Vis titration studies (without the background concentration of the host) for the co-system **4•2** in $CHCl_3$/ DMSO (99:1).

Photophysical properties

A preliminary photophysical studies of the co-systems **4•2/3** and their individual components were undertaken in $CHCl_3$ solutions (See Supporting Information Section S5). The results are summarised in Table 1 and overlaid emission spectra of the new complexes are illustrated in Figure 9. Complex **4** is a green emitter (Figure 8a) with a λ_{PL} at 490 nm and a shoulder peak at 514 nm and PL quantum yield 2.6% in $CHCl_3$.

Table 1. Photophysical Data for 2, 3, 4 and co-systems 4•2/3.

Compound	λ_{PL}/ nm[a]	Φ_{PL} [b] *(ex: 360 nm)*	*CIE / x,y*[c]
2	423	8.1	0.15, 0.05
3	418,442	16.7	0.16,0.07
4	490,514	2.6	0.24,0.53
4•2	423	4.3	0.17, 0.14
4•3	416,440	8.5	0.17,0.07

[a]Solution data are reported in $CHCl_3$, excited at 360 nm. For measurements of co systems, 1:1 ratio of iridium complex **4** and compound **2/3** applied. [b]All sample excited at 360 nm. PLQY determined by direct method, using integrating sphere [c]CIE 1931 coordinates of $CHCl_3$ solutions, excited at 360 nm.

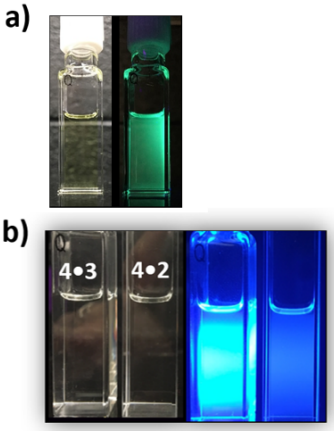

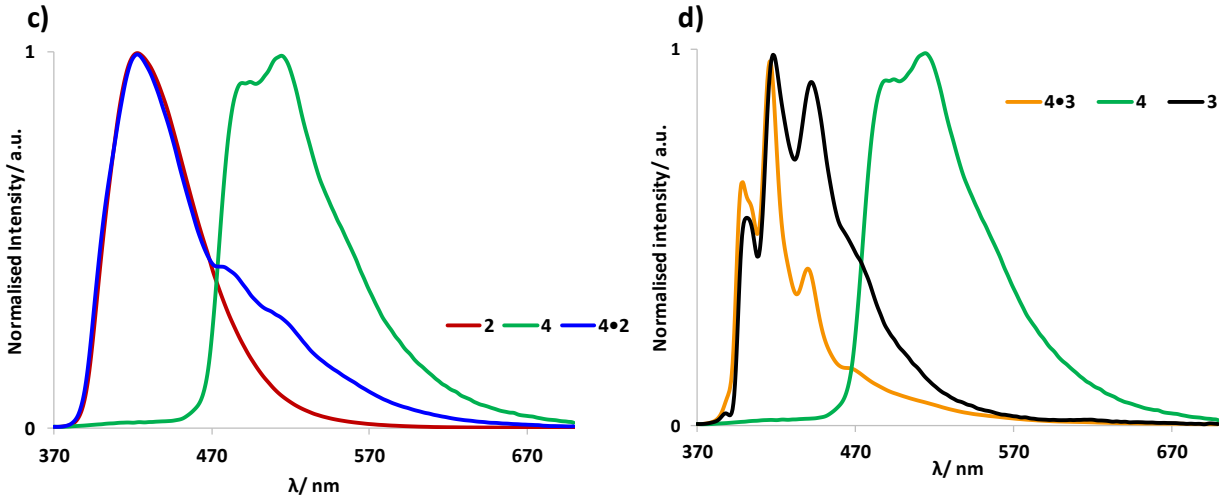

Figure 9. a) Photos of $CHCl_3$ solutions of complex **4**, in quartz cuvettes under ambient light (left) and under 365 nm UV light (right) b) Photos of $CHCl_3$ solutions of co-systems **4•3** and **4•2** in quartz cuvettes under ambient light (top) and under 365 nm UV light (bottom) c) Normalised emission spectra of solution ($CHCl_3$, $1x10^{-5}$ M) of **2** (red), **4** (green), **4•2** (blue) d) Normalised emission spectra of solution ($CHCl_3$, $1x10^{-5}$ M) of **3** (black), **4** (green), **4•3** (orange).

As mentioned in the literature,[60] there is still high demand for efficient blue phosphorescent Ir (III) complexes, especially for their application as emitters in phosphorescent organic light emitting diodes (PhOLEDs). Their synthesis is often based on the substitution of the N^N ligands, carrying an electron withdrawing group.[61-63] An elegant example of design and synthesis of two new sky-blue iridium complexes was recently published by Wang and co-workers.[64] They examined the optimal ^{3}LC and ^{3}MLCT/^{3}LLCT transitions in order to control the molecule design strategy. Our approach suggests that the chromaticity of the heteroleptic

iridium complexes with precisely organised arrangements of ligands can be tuned through H-bonding. As a result, controlled self-assembly provides a way for developing phosphorescent iridium complexes emitting blue colour (Figure 9b) without the need to alter the N^N ligands attached to the metal centre. We are now currently conducting more comprehensive analysis on this class of material in our research group.

Conclusion

In summary, we have presented synthesis and binding studies of four stable hydrogen bonded systems with different arrangements through ^{1}H NMR and UV-Vis analysis. The free rotation of thiourea based derivative was inhibited through incorporation of metal into the structure. To this end, we also have successfully demonstrated design, synthesis and characterisation of a new heteroleptic iridium complex **4** using 2-phenylpyridinato C^N ligands and benzimidazolate-linked thiourea ligand. We have further explored their binding properties with fused hetero-*n*-acenes. This study demonstrates a novel methodology for the enhancement of stability in triple hydrogen bonded systems and extended the library of H-bonded heterodimers based on iridium. The examined stabilities of these assemblies make them ideal building blocks for the preparation of supramolecular polymers or for applications in which complementary H-bonded association is desirable. Moreover, we reported the photoluminescence properties of complex **4** and its respective heterodimers when combined with **2** and **3** and further efforts in this area will be reported in due course.

Notes

The authors declare no competing financial interests. The raw data which underpins this work is available at https://doi.org/10.25545/WHD3KC.

Acknowledgments

BAB is grateful for financial support from University of New Brunswick, New Brunswick Foundation for Innovation (NBIF), and the Natural Science and Engineering Council of Canada (NSERC).

References

(1) Eberhardt ES, Raines RT. Amide-Amide and Amide-Water Hydrogen Bonds: Implications for Protein Folding and Stability. *J Am Chem Soc.* **1994**; 116(5):2149–2150.

(2) Fernández, A.; Sosnick, T. R.; Colubri, A. Dynamics of Hydrogen Bond Desolvation in Protein Folding. *J. Mol. Biol.* **2002**, *321* (4), 659–675 DOI:10.1016/S0022-2836(02)00679-4.

(3) Steiner, T. The Hydrogen Bond in the Solid State. *Angew. Chemie Int. Ed.* **2002**, *41* (1), 48–76 DOI: 10.1002/1521-3773(20020104)41.

(4) G. A. Jeffrey, *An introduction to hydrogen bonding*, Oxford university press New York, **1997**, ISBN: 0195095499, 9780195095494 .

(5) Sijbesma, R. P.; Meijer, E. W. Quadruple Hydrogen Bonded Systems. *Chem. Commun.* **2003**, No. 1, 5–16 DOI: 10.1039/B205873C.

(6) Bell, T. W.; Hou, Z. A Hydrogen-Bonding Receptor That Binds Urea with High Affinity. *Angew. Chemie Int. Ed. English* **1997**, *36* (13-14), 1536–1538 DOI: doi:10.1002/anie.199715361.

(7) Vijayakumar, V. N.; Mohan, M. L. N. M. Synthesis and Characterization of Double Hydrogen Bonded Ferroelectric Liquid Crystals Exhibiting Reentrant Smectic Ordering. *Ferroelectrics* **2009**, *392* (1), 81–97 DOI: 10.1080/00150190903412556.

(8) Pihko, P. M. Activation of Carbonyl Compounds by Double Hydrogen Bonding: An Emerging Tool in Asymmetric Catalysis. *Angew. Chemie Int. Ed.* **2004**, *43* (16), 2062–2064 DOI: 10.1002/anie.200301732.

(9) Burrows, A. D.; Chan, C.-W.; Chowdhry, M. M.; McGrady, J. E.; Mingos, D. M. P. Multidimensional Crystal Engineering of Bifunctional Metal Complexes Containing

Complementary Triple Hydrogen Bonds. *Chem. Soc. Rev.* **1995**, *24* (5), 329–339 DOI: 10.1039/CS9952400329.

(10) Hoeben, F. J. M.; Pouderoijen, M. J.; Schenning, A. P. H. J.; Meijer, E. W. Energy Transfer in Chiral Co-Assemblies of Triple Hydrogen-Bonded Oligo(p-Phenylene Vinylene)s and Porphyrin. *Org. Biomol. Chem.* **2006**, *4* (24), 4460–4462 DOI: 10.1039/B612790H.

(11) Djurdjevic, S.; Leigh, D. A.; McNab, H.; Parsons, S.; Teobaldi, G.; Zerbetto, F. Extremely Strong and Readily Accessible AAA−DDD Triple Hydrogen Bond Complexes. *J. Am. Chem. Soc.* **2007**, *129* (3), 476–477 DOI: 10.1021/ja067410t.

(12) Blight, B. A.; Camara-Campos, A.; Djurdjevic, S.; Kaller, M.; Leigh, D. A.; McMillan, F. M.; McNab, H.; Slawin, A. M. Z. AAA−DDD Triple Hydrogen Bond Complexes. *J. Am. Chem. Soc.* **2009**, *131* (39), 14116–14122 DOI: 10.1021/ja906061v.

(13) Blight, B. A.; Hunter, C. A.; Leigh, D. A.; McNab, H.; Thomson, P. I. T. An AAAA–DDDD Quadruple Hydrogen-Bond Array. *Nat. Chem.* **2011**, *3*, 244.

(14) Han, Y.-F.; Chen, W.-Q.; Wang, H.-B.; Yuan, Y.-X.; Wu, N.-N.; Song, X.-Z.; Yang, L. An AAA–DDD Triply Hydrogen-Bonded Complex Easily Accessible for Supramolecular Polymers. *Chem. – A Eur. J.* **2014**, *20* (51), 16980–16986 DOI: 10.1002/chem.201404996.

(15) Sartorius, J.; Schneider, H.-J. A General Scheme Based on Empirical Increments for the Prediction of Hydrogen-Bond Associations of Nucleobases and of Synthetic Host–Guest Complexes. *Chem. Eur. J.* **1996**, *2* (11), 1446–1452 DOI: 10.1002/chem.19960021118.

(16) Jorgensen, W. L.; Pranata, J. Importance of Secondary Interactions in Triply Hydrogen Bonded Complexes: Guanine-Cytosine vs Uracil-2, 6-Diaminopyridine. *J. Am. Chem. Soc.* **1990**, *112* (5), 2008–2010 DOI: 10.1021/ja00161a061.

(17) Pranata, J.; Wierschke, S. G.; Jorgensen, W. L. OPLS Potential Functions for Nucleotide Bases. Relative Association Constants of Hydrogen-Bonded Base Pairs in Chloroform. *J. Am. Chem. Soc.* **1991**, *113* (8), 2810–2819 DOI: 10.1021/ja00008a002.

(18) Murray, T. J.; Zimmerman, S. C. New Triply Hydrogen Bonded Complexes with Highly Variable Stabilities. *J. Am. Chem. Soc.* **1992**, *114* (10), 4010–4011 DOI: 10.1021/ja00036a079.

(19) Zimmerman, S. C.; Murray, T. J. Hydrogen Bonded Complexes with the AA·DD, AA·DDD, and AAA·DD Motifs: The Role of Three Centered (Bifurcated) Hydrogen Bonding. *Tetrahedron Lett.* **1994**, *35* (24), 4077–4080 DOI: https://doi.org/10.1016/S0040-4039(00)73116-9.

(20) Papmeyer, M.; Vuilleumier, C. A.; Pavan, G. M.; Zhurov, K. O.; Severin, K. Molecularly Defined Nanostructures Based on a Novel AAA–DDD Triple Hydrogen-Bonding Motif. *Angew. Chemie Int. Ed.* **2016**, *55* (5), 1685–1689 DOI: 10.1002/anie.201510423.

(21) Han, Y.-F.; Chen, W.-Q.; Wang, H.-B.; Yuan, Y.-X.; Wu, N.-N.; Song, X.-Z.; Yang, L. *Chem. – A Eur. J.* **2014**, 20 (51), 16980–16986 DOI: 10.1002/chem.201404996.

(22) Mendez, I. J. L.; Wang, H.-B.; Yuan, Y.-X.; Wisner, J. A. Supramolecular Polymers Based on Non-Coplanar AAA-DDD Hydrogen-Bonded Complexes. *Macromol. Rapid Commun.* **2018**, *39* (5), 1700619 DOI: 10.1002/marc.

(23) Caltagirone, C.; Hiscock, J. R.; Hursthouse, M. B.; Light, M. E.; Gale, P. A. 1,3-Diindolylureas and 1,3-Diindolylthioureas: Anion Complexation Studies in Solution and the Solid State. *Chem. – A Eur. J.* **2008**, *14* (33), 10236–10243 DOI: 10.1002/chem.200801639.

(24) Murali, M. G.; Vishnumurthy, K. A.; Seethamraju, S.; Ramamurthy, P. C. Colorimetric Anion Sensor Based on Receptor Having Indole- and Thiourea-Binding Sites. *RSC Adv.* **2014**, *4* (39), 20592–20598 DOI: 10.1039/C4RA01555J.

(25) Emami Khansari, M.; Johnson, C. R.; Basaran, I.; Nafis, A.; Wang, J.; Leszczynski, J.; Hossain, M. A. Synthesis and Anion Binding Studies of Tris(3-Aminopropyl)Amine-Based Tripodal Urea and Thiourea Receptors: Proton Transfer-Induced Selectivity for Hydrogen Sulfate over Sulfate. *RSC Adv.* **2015**, *5* (23), 17606–17614 DOI: 10.1039/C5RA01315A.

(26) Jiménez Blanco, J. L.; Bootello, P.; Benito, J. M.; Ortiz Mellet, C.; García Fernández, J. M. Urea-, Thiourea-, and Guanidine-Linked Glycooligomers as Phosphate Binders in Water. *J. Org. Chem.* **2006**, *71* (14), 5136–5143 DOI: 10.1021/jo060360q.

(27) Chung, Y. K.; Ha, S.; Woo, T. G.; Kim, Y. D.; Song, C.; Kim, S. K. Binding Thiourea Derivatives with Dimethyl Methylphosphonate for Sensing Nerve Agents. *RSC Adv.* **2019**, *9* (19), 10693–10701 DOI: 10.1039/C9RA00314B.

(28) Wenzel, M.; Light, M. E.; Davis, A. P.; Gale, P. A. Thiourea Isosteres as Anion Receptors and Transmembrane Transporters. *Chem. Commun.* **2011**, *47* (27), 7641–7643. https://doi.org/10.1039/C1CC12439K.

(29) Kado, S.; Otani, H.; Nakahara, Y.; Kimura, K. Highly Selective Recognition of Acetate and Bicarbonate by Thiourea-Functionalised Inverse Opal Hydrogel in Aqueous Solution. *Chem. Commun.* **2013**, *49* (9), 886–888 DOI: 10.1039/C2CC38052H.

(30) Wang, L.; Wu, Y.; Shan, G.-G.; Geng, Y.; Zhang, J.-Z.; Wang, D.-M.; Yang, G.-C.; Su, Z.-M. The Influence of the Diphenylphosphoryl Moiety on the Phosphorescent Properties of Heteroleptic Iridium (III) Complexes and the OLED Performance: A Theoretical Study. *J. Mater. Chem. C* **2014**, *2* (16), 2859–2868 DOI: 10.1039/C3TC31831A.

(31) Henwood, A. F.; Antón-García, D.; Morin, M.; Rota Martir, D.; Cordes, D. B.; Casey, C.; Slawin, A. M. Z.; Lebl, T.; Bühl, M.; Zysman-Colman, E. Conjugated, Rigidified Bibenzimidazole Ancillary Ligands for Enhanced Photoluminescence Quantum Yields of Orange/Red-Emitting Iridium(III) Complexes. *Dalt. Trans.* **2019** DOI: 10.1039/C9DT00423H.

(32) Kessler, F.; Watanabe, Y.; Sasabe, H.; Katagiri, H.; Nazeeruddin, M. K.; Grätzel, M.; Kido, J. High-Performance Pure Blue Phosphorescent OLED Using a Novel Bis-Heteroleptic Iridium(III) Complex with Fluorinated Bipyridyl Ligands. *J. Mater. Chem. C* **2013**, *1* (6), 1070–1075 DOI: 10.1039/C2TC00836J.

(33) Chau, N.-Y.; Ho, P.-Y.; Ho, C.-L.; Ma, D.; Wong, W.-Y. Color-Tunable Thiazole-Based Iridium (III) Complexes: Synthesis, Characterization and Their OLED Applications. *J. Organomet. Chem.* **2017**, *829*, 92–100 DOI: https://doi.org/10.1016/j.jorganchem.2016.11.018.

(34) Galán, L. A.; Cordes, D. B.; Slawin, A. M. Z.; Jacquemin, D.; Ogden, M. I.; Massi, M.; Zysman-Colman, E. Analyzing the Relation between Structure and Aggregation Induced Emission (AIE) Properties of Iridium(III) Complexes through Modification of Non-Chromophoric Ancillary Ligands. *Eur. J. Inorg. Chem.* **2019**, *2019* (2), 152–163 DOI: 10.1002/ejic.201801118.

(35) Su, N.; Yang, H.; Shen, C.-Z.; Yan, Z.-P.; Chen, Z.-X.; Zheng, Y.-X. Rapid Room Temperature Synthesis of Red Iridium (III) Complexes with Ir-S-P-S Structures for Efficient OLEDs. *J. Mater. Chem. C* **2019** DOI: 10.1039/C9TC01564G.

(36) Lu, G.-Z.; Tu, Z.-L.; Liu, L.; Zhang, W.-W.; Zheng, Y.-X. Fast Synthesis of Iridium (III) Complexes with Sulfur Containing Ancillary Ligand for High-Performance Green OLEDs with EQE over 31%. *J. Mater. Chem. C* **2019** DOI: 10.1039/C9TC01397K.

(37) Su, N.; Yang, H.; Zheng, Y.-X.; Chen, Z.-X. Sulfur Atom Contained Ligands Induced Rapid Room Temperature Synthesis of Red Iridium (III) Complexes with Ir-S-P-S Structures for OLEDs. *New J. Chem.* **2019** DOI: 10.1039/C9NJ01599J.

(38) Sheldrick, G. M. SHELXT: Integrated Space-Group and Crystal-Structure Determination. *Acta Crystallogr*., Sect. A: Found. Adv. **2015**, 71, 3−8.

(39) Sheldrick, G. M. Crystal Structure Refinement with SHELXL. *Acta Crystallogr*., Sect. C: Struct. Chem. **2015**, 71, 3 −8.

(40) Dolomanov, O. V.; Bourhis, L. J.; Gildea, R. J.; Howard, J. A. K.; Puschmann, H. OLEX2: A Complete Structure Solution, Refinement and Analysis Program. *J. Appl. Crystallogr*. **2009**, 42, 339 −341.

(41) Supramolecular BindFit. www.supramolecular.org.

(42) Nonoyama, M. Benzo[h]quinolin-10-yl-N Iridium (III) Complexes. *Bull. Chem. Soc. Jpn*. **1974**, 47, 767 −768.

(43) Vig, R.; Mao, C.; Venkatachalam, T. K.; Tuel-Ahlgren, L.; Sudbeck, E. A.; Uckun, F. M. Rational Design and Synthesis of Phenethyl-5-Bromopyridyl Thiourea Derivatives as Potent NonNucleoside Inhibitors of HIV Reverse Transcriptase. *Bioorg. Med. Chem*. **1998**, 6, 1789 −1797.

(44) Balónová, B.; Martir, D. R.; Clark, E. R.; Shepherd, H. J.; Zysman-Colman, E.; Blight, B. A. Influencing the Optoelectronic Properties of a Heteroleptic Iridium Complex by Second-Sphere H-Bonding Interactions. *Inorg. Chem.* **2018**, *57* (14), 8581–8587 DOI: 10.1021/acs.inorgchem.8b01326.

(45) Pelphrey, P. M.; Popov, V. M.; Joska, T. M.; Beierlein, J. M.; Bolstad, E. S. D.; Fillingham, Y. A.; Wright, D. L.; Anderson, A. C. Highly Efficient Ligands for Dihydrofolate Reductase from

Cryptosporidium Hominis and Toxoplasma Gondii Inspired by Structural Analysis. *J. Med. Chem.* 2007, 50, 940 −950.

(46) Blight, B. A.; Camara-Campos, A.; Djurdjevic, S.; Kaller, M.; Leigh, D. A.; McMillan, F. M.; McNab, H.; Slawin, A. M. Z. AAA − DDD Triple Hydrogen Bond Complexes. *J. Am. Chem. Soc.* **2009**, 131, 14116 −14122.

(47) Rowland, R. S.; Taylor, R. Intermolecular Nonbonded Contact Distances in Organic Crystal Structures: Comparison with Distances Expected from van Der Waals Radii. *J. Phys. Chem.* **1996**, 100, 7384 − 7391.

(48) Bordwell, F. G.; Algrim, D. J.; Harrelson, J. A. The Relative Ease of Removing a Proton, a Hydrogen Atom, or an Electron from Carboxamides versus Thiocarboxamides. *J. Am. Chem. Soc.* **1988**, *110* (17), 5903–5904 DOI: 10.1021/ja00225a054.

(49) Sundareswari,M.;Rajagopalan, M. Study of the Electronic Structure and Physical Properties of the Iridium based Intermetallic Compounds Under Pressure. *Int. J. Mod. Phys. B* **2005**, *19* (31), 4587–4604. https://doi.org/10.1142/S0217979205032966.

(50) Ren, X.; Giesen, D. J.; Rajeswaran, M.; Madaras, M. Synthesis, Characterization, and Physical Properties of Cyclometalated Iridium(III) Complexes with 2-Phenylthiophene or 2-Phenylfuran Ligands. *Organometallics* **2009**, *28* (20), 6079–6089. https://doi.org/10.1021/om9006246.

(51) Esteruelas, M. A.; Oñate, E.; Palacios, A. U. Selective Synthesis and Photophysical Properties of Phosphorescent Heteroleptic Iridium(III) Complexes with Two Different Bidentate Groups and Two Different Monodentate Ligands. *Organometallics* **2017**, *36* (9), 1743–1755. https://doi.org/10.1021/acs.organomet.7b00108.

(52) Li, G.-N.; Dou, S.-B.; Zheng, T.; Chen, X.-Q.; Yang, X.-H.; Wang, S.; Sun, W.; Chen, G.-Y.; Mo, Z.-R.; Niu, Z.-G. Orange-Red Phosphorescent Iridium(III) Complexes Bearing Bisphosphine Ligands: Synthesis, Photophysical and Electrochemical Properties, and DFT Calculations. *Organometallics* **2018**, *37* (1), 78–86. https://doi.org/10.1021/acs.organomet.7b00740.

(53) Tamura, Y.; Hisamatsu, Y.; Kazama, A.; Yoza, K.; Sato, K.; Kuroda, R.; Aoki, S. Stereospecific Synthesis of Tris-Heteroleptic Tris-Cyclometalated Iridium(III) Complexes via Different Heteroleptic Halogen-Bridged Iridium(III) Dimers and Their Photophysical Properties. *Inorg. Chem.* **2018**, *57* (8), 4571–4589. https://doi.org/10.1021/acs.inorgchem.8b00323.

(54) Li, Q.; Zhang, X.; Cao, Y.; Shi, C.; Tao, P.; Zhao, Q.; Yuan, A. An Oxygen-Bridged Triarylamine Polycyclic Unit Based Tris-Cyclometalated Heteroleptic Iridium(Iii) Complex: Correlation between the Structure and Photophysical Properties. *Dalt. Trans.* **2019**, *48* (14), 4596–4601. https://doi.org/10.1039/C9DT00344D.

(55) Kong, D.; Tian, M.; Guo, L.; Liu, X.; Zhang, S.; Song, Y.; Meng, X.; Wu, S.; Zhang, L.; Liu, Z. Novel Iridium(III) Iminopyridine Complexes: Synthetic, Catalytic, and in Vitro Anticancer

Activity Studies. *JBIC J. Biol. Inorg. Chem.* **2018**, *23* (5), 819–832. https://doi.org/10.1007/s00775-018-1578-0.

(56) Chen, W.; Liu, F.-X.; Gong, W.; Zhou, Z.; Gao, H.; Shi, J.; Wu, B.; Yi, W. Hydroxyl Group-Prompted and Iridium(III)-Catalyzed Regioselective C−H Annulation of N-Phenoxyacetamides with Propargyl Alcohols. *Adv. Synth. Catal.* **2018**, *360* (13), 2470–2475. https://doi.org/10.1002/adsc.201800322.

(57) Zhong, R.-L.; Sakaki, S. Sp3 C–H Borylation Catalyzed by Iridium(III) Triboryl Complex: Comprehensive Theoretical Study of Reactivity, Regioselectivity, and Prediction of Excellent Ligand. *J. Am. Chem. Soc.* **2019**. https://doi.org/10.1021/jacs.9b01767.

(58) Djurdjevic, S.; Leigh, D. A.; McNab, H.; Parsons, S.; Teobaldi, G.; Zerbetto, F. Extremely Strong and Readily Accessible AAA−DDD Triple Hydrogen Bond Complexes. *J. Am. Chem. Soc.* **2007**, *129* (3), 476–477 DOI: 10.1021/ja067410t.

(59) Yang, C.-H.; Cheng, Y.-M.; Chi, Y.; Hsu, C.-J.; Fang, F.-C.; Wong, K.-T.; Chou, P.-T.; Chang, C.-H.; Tsai, M.-H.; Wu, C.-C. Blue-Emitting Heteroleptic Iridium(III) Complexes Suitable for High-Efficiency Phosphorescent OLEDs. *Angew. Chemie Int. Ed.* **2007**, *46* (14), 2418–2421 DOI: 10.1002/anie.200604733.

(60) Kim, J.-B.; Han, S.-H.; Yang, K.; Kwon, S.-K.; Kim, J.-J.; Kim, Y.-H. Highly Efficient Deep-Blue Phosphorescence from Heptafluoropropyl-Substituted Iridium Complexes. *Chem. Commun.* **2015**, *51* (1), 58–61 DOI: 10.1039/C4CC07768G.

(61) Henwood, A. F.; Bansal, A. K.; Cordes, D. B.; Slawin, A. M. Z.; Samuel, I. D. W.; Zysman-Colman, E. Solubilised Bright Blue-Emitting Iridium Complexes for Solution Processed OLEDs. *J. Mater. Chem. C* **2016**, *4* (17), 3726–3737 DOI: 10.1039/C6TC00151C.

(62) Li, X.; Zhang, J.; Zhao, Z.; Wang, L.; Yang, H.; Chang, Q.; Jiang, N.; Liu, Z.; Bian, Z.; Liu, W.; Lu, Z.; Huang, C. Deep Blue Phosphorescent Organic Light-Emitting Diodes with CIEy Value of 0.11 and External Quantum Efficiency up to 22.5%. *Adv. Mater.* **2018**, *30* (12), 1705005 DOI: 10.1002/adma.201705005.

(63) Du, M.; Wang, Y.; Wang, J.; Chen, S.; Wang, Z.; Wang, S.; Bai, F.; Liu, Y.; Wang, Y. Novel Sky Blue Heteroleptic Iridium(III) Complexes with Finely-Optimized Emission Spectra for Highly Efficient Organic Light-Emitting Diodes. *J. Mater. Chem. C* **2019** DOI: 10.1039/C9TC00918C.